Journal of Coastal Research	17	1	162–172	West Palm Beach, Florida	Winter 2001

A System for Measuring Horizontal Sand Transport by Currents

Georges Chapalain and Laurent Thais

Laboratoire de Sédimentologie et Géodynamique
Université des Sciences et Technologies de Lille
UMR-CNRS 8577
Bâtiment SN5
59655 Villeneuve d'Ascq, France

ABSTRACT

CHAPALAIN, G. and THAIS, L., 2001. A system for measuring horizontal sand transport by currents. *Journal of Coastal Research,* 17(1), 162–172. West Palm Beach (Florida), ISSN 0749-0208.

We describe a new sand trapping system which enables measurement of horizontal transport rates of suspended sand in the benthic boundary layer of multidirectional unsteady currents. A field test carried out through a tidal cycle in the tide-dominated shallow waters of the eastern English Channel demonstrates the utility of the new system. Amounts of sediment trapped in the different directions are compared with predictions by a simple theoretical approach. The applicability of the new system is then discussed. The net total transport rates and the net transport rates as a function of grain size appear complicated. They are characterized by significant cross-shore contributions maybe related to the cross-shore heterogeneity of the application area in terms of hydrodynamics and sediment suspension.

Although still pledged with uncertainties about directional sensitivity of the traps and induced flow disturbances, this new system appears a promising tool for future studies of sediment transport in coastal areas.

ADDITIONAL INDEX WORDS: *Measurement technique, sand trap, sediment transport, bottom.*

INTRODUCTION

The relationship between sediment fluxes and hydrodynamic and sedimentary factors remains to date poorly understood. Measurements of sediment fluxes in the bottom boundary layer are still necessary to improve our basic understanding of sediment movement in the hope of developing predictive engineering techniques for estimating transport rates and morphologic evolution.

Over the past two decades, many instruments for measuring sediment transport have been developed. A first category of instruments uses indirect measurements and operates on the principle of interactions between sediment load and electromagnetic, or acoustic waves (*e.g.,* HUNTLEY, 1982; HORIKAWA, 1988; BASINSKI, 1989). These systems, which measure separately the suspended sediment concentration and the transporting velocity, have high temporal resolution. Eventhough recent acoustic devices are capable of measuring grain size distribution (*e.g.,* HAY and SHENG, 1992), the response of most of them to sedimentological parameters, such as grain size distribution and composition, as well as particulate and dissolved organic matter, remains difficult to establish. Additionally, these electronic devices are expensive and require careful calibration.

A second sort of instruments is provided by sediment trapping systems which allow direct measurements without preliminary calibration. Suspended sand traps fall themselves in two sub-types, namely settling traps and sieving traps.

98269 received 30 November 1998; accepted in revision 25 April 2000.

Settling-type traps are designed so that sediments are deposited in a receptacle. One of the first devices of this kind was the well-known bamboo sampler developed by FUKUSHIMA and MIZOGUCHI (1958). This device is a bamboo pole with small hollows between adjacent joints used as receptacles. Two holes facing each other serve as an entrance to the sand-fluid mixture, and as an exit for the fluid flow. More recently, sediment traps similar to bamboo traps were constructed using segmented plastic pipes by BASINSKI and LEWANDOWSKI (1974), KAJIMA (1980), ANTSYFEROV *et al.* (1983), and SCHOONEES (1991). A more sophisticated settling trap is the 'Delft Bottle' (as referenced in MCCAVE, 1979 and GRAF, 1984). This bottle-shaped device consists of a nozzle that opens into a chamber with holes in its rear plate. The water-sediment mixture entering the nozzle slows down in the inner chamber, allowing the suspended particles to settle, while the water exits through the rear holes.

Many kinds of suspended sand traps using sieves have been designed. SATO (1957) and HOM-MA *et al.* (1960) developed traps made of steel mesh tubes. JAMES and BRENNINKMEYER (1971) proposed a device with a nozzle connected to a cylinder, and a steel mesh at the rear. KAJIMA (1980) designed a multi-level trapping system consisting of a cylinder partitioned into five levels, themselves divided in four compartments with steel mesh windows. BECCHI *et al.* (1981) proposed a device using a paper filter bag inserted into a drilled cage. Flexible collection bags called streamers attached to a nozzle have also been used to reduce flow disturbances caused by rigid structures. NAGATA (1964) used a cotton cloth

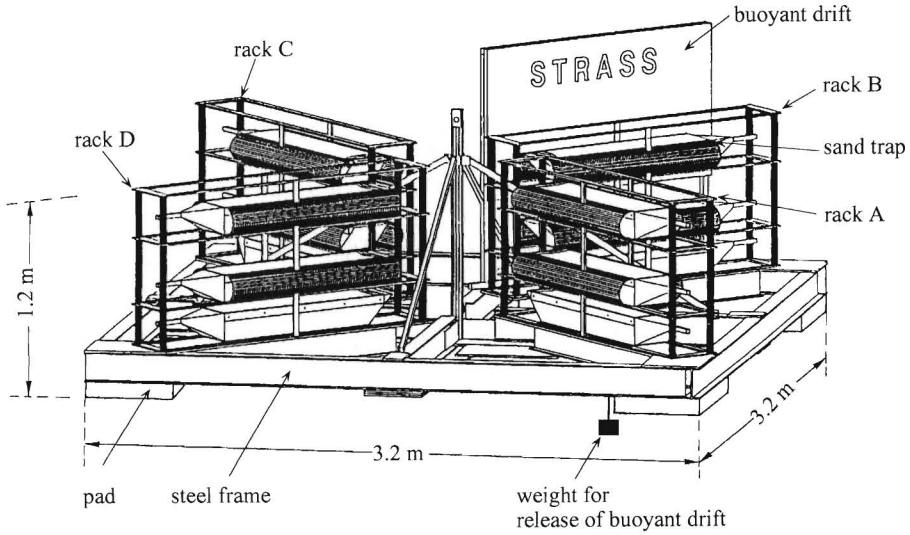

Figure 1. Schematic diagram of the system for trapping suspended sand (STRASS).

streamer, KATTORI (1982) a plankton net, which KRAUS (1987) replaced by a polyester monofilament sieve cloth. KATTORI (1983) improved the device by installing a door designed to swing open on the inflow and to shut at flow reversals, preventing loss of trapped material. KRAUS (1987) mounted a series of these streamer traps on a rack to measure the vertical distribution of suspended sediment transport rate.

The applicability of traps in complex coastal environments characterized by strong multi-directional unsteady currents must respect two major constraints (1) such devices must not trap sediments coming from opposite directions; (2) the trapping efficiency must remain optimal at highest flow velocities during deployment. The second point is because varying efficiency does not permit determination of the time-integrated sediment flux from the total mass of trapped sediment.

Although very useful, prior traps have shown limitations with regard to the above constraints. Traps using sieves have encountered severe problems of flow disturbances under high fluid regimes (HORIKAWA, 1988). They are also subject to meshes plugging up. For streamer traps, sediment filling of the streamer modifies the trap behaviour, and thereby its trapping efficiency. Prior settling-type traps have also been fraught with partial, and sometimes unknown, sediment-trapping efficiency, as well as high sensivity to reversing flows.

The present paper introduces a new trapping system with acronym STRASS—System for TRApping Suspended Sand. STRASS was designed to measure the vertical distribution of the horizontal transport rates of suspended sand within the benthic boundary layer of multi-directional unsteady currents. The system can operate in macrotidal environments (spring-tidal range > 4 m) characterized by strong sediment transport. The system can also operate in areas subject to quasi-steady currents such as wind-induced currents. STRASS is an assemblage of twelve recently-developed suspended sand traps described and tested in CHAPALAIN (1998).

The paper is organized as follows: Section 2 describes the design and operation of STRASS, and briefly recalls the characterics of one individual sand trap. The first deployment of STRASS in the field and the general nature of data obtained are given in Section 3 and discussed in Section 4. Section 5 presents the summary and conclusions of this work.

THE SYSTEM FOR TRAPPING SUSPENDED SAND

The complete system STRASS—System for TRApping Suspended Sand was designed to collect sediment within the bottom boundary layer. It is shown in Figure 1. STRASS is a steel frame hosting a series of twelve sand traps.

The Steel Frame

The steel frame of STRASS is a 3.2 m $\times$ 3.2 m square base with a 1.6 m high central lifting rod (Figure 1). The frame dimensions and its shape make it relatively easy to transport and handle on a ship, with minimal risk of damage at deployment owing to the overall stability of the platform. The frame is equipped with four 0.07 m-high pads to reduce disturbance of the bedload transport.

Four vertical racks constructed of stainless rods are mounted along the diagonals of the frame. They are labelled A,B,C,D counter clockwise as shown in Figure 1. Each rack hosts an array of three horizontally-mounted suspended sediment traps. The central axes of the trap entrance are respectively 0.37, 0.64 and 0.92 m above the sea-bed. These levels will be labelled 1, 2, and 3, corresponding to the respective bottom, middle, and top elevations. The space between the traps and the racks permits flow circulation. The individual sand traps are described below.

The Suspended Sand Traps

The suspended sand trap designed for STRASS incorporates a number of features which are intended to meet re-

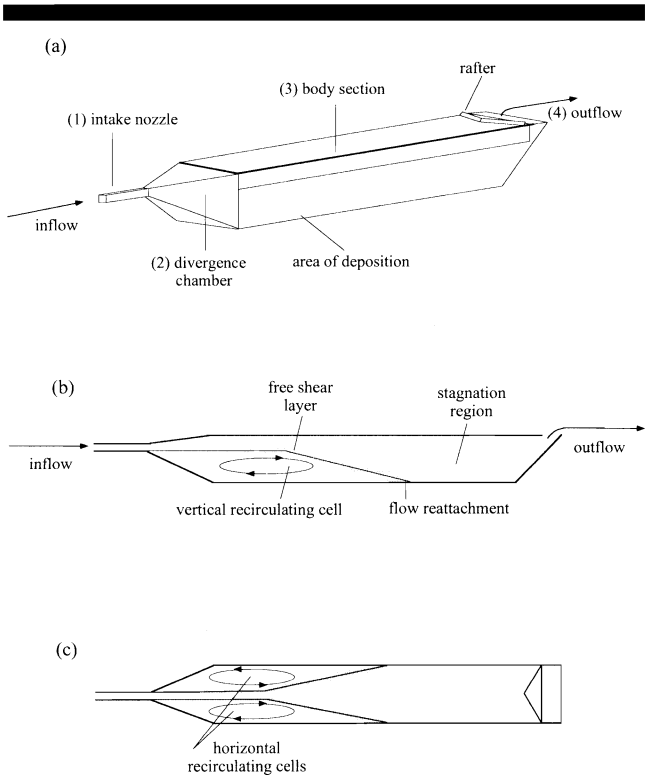

Figure 2. Schematic diagram of the mono-directional suspended sand trap and its inner flow patterns. (a) side view (b) vertical slice (c) horizontal slice.

quirements of measuring in strong multi-directional unsteady flows. The trap operates on the dual-principle of (1) settling activated by a gradual reduction of fluid and sediment particle velocities and (2) trapping of sediment particles by recirculating and quasi-stagnant flows. The retained settling-type trap lessens problems of flow disturbance associated with sieving-type traps.

Full details on the present sand trap together with efficiency tests can be found in CHAPALAIN (1998). Here, we will briefly recall the main elements of the trap displayed in Figure 2. From left to right in this figure, *i.e.* following the flow downstream, the trap is divided in four elements, namely,

(1) an intake nozzle,
(2) a divergence chamber,
(3) a body section,
(4) an outflow.

The aim of the intake nozzle (0.17 m long with a square section 0.02 m × 0.02 m) is to move upstream the flow entrance in order to minimize flow disturbances caused by the trap body. The nozzle opens into a divergence chamber 0.2 m in length. It is connected to the rectangular body section 0.2 m × 0.14 m, and 0.9 m in length which serves as a receptacle for trapped particles. Finally, the trap exit is a 45° inclined plane that opens into an exhaust vent (0.02 m × 0.2 m) located in the rear part of the trap lid. In horizontal section, the divergence chamber is symmetrical and has a large opening angle. In vertical section, it is asymmetrical and characterized by a large lower half-divergence slope (½) and a narrow upper half-divergence slope ($1/10$).

The flow patterns in the trap are shematized in Figure 2b (vertical slice) and Figure 2c (horizontal slice). The first action of the divergence chamber is to reduce the mean flow. In addition, the divergence chamber and the upstream part of the body section produce a vertically separated flow. This flow divides in a free shear layer, a recirculating cell and a reattachment/quasi-stagnation region in the lower part of the body (Figure 2b). In the upper part of the divergence chamber, we have two symmetrical horizontally separated flows (Figure 2c).

The vertical recirculation cell has downward mean velocities which, combined with gravity settling, increase trapping efficiency. The narrow upper half-divergence prevents another free shear layer to develop in the upper part of the body section, thus minimizing particle diffusion towards the trap lid. Downstream of the separated flow, sediment particles remaining in suspension in the free stream and the shear layer settle in the quasi-stagnation region.

The exit closes the trap on the rear, retains deposited particles and ensures mono-directionality under adverse ambient flow. A deflector in the form of a rafter located just upstream of the exit evacuates sideways particles having sedimented on top of the trap. It is completed by a plate located above the exit to prevent direct vertical sedimentation through the opening.

The design of the trap was first chosen from considerations pertaining to the separated flow on which rests the trapping principle. The dimensions were later refined and adjustments made on the basis of flow visualizations in a laboratory channel circulating fluoresceined water. In that respect, it should be mentioned that the intake nozzle was added afterwards, since flow disturbances without any nozzle were caused just upstream of the trap by the divergence chamber. The section of the nozzle is large with respect to sediment grains, but small with respect to the large energy containing eddies of a seabed boundary layer, which means the inevitable slowing down of the ambient flow occurs downstream of the collecting point. Also, the small size of the nozzle induces a more significant venturi effect in the divergence chamber, which improves trapping efficiency. In the same time, this avoids trapping too large quantity of sediments. Laboratory tests consisting in releasing glass spheres and natural sediment in the intake nozzle proved the trapping efficiency of the device. The range of applicability of the trap was also determined on the basis of numerical computations of particle trajectories released in the intake nozzle under laboratory and natural conditions (CHAPALAIN, 1998). This study showed the trap was almost 'totally efficient', with a 99% trapping efficiency for particles larger than 125 μm in diameter and current speeds up to 1.4 m/s, and 97% for particles larger than 100 μm and current speeds up to 1.1 m/s.

Operation

To begin a cycle of use, STRASS is slowly lowered towards the sea-bed. The deployment should be preferably carried out at times of well-established currents. A buoyant drift, main-

tained with a small weight hanging below the frame level, forces racks B and D to align with the current while lowering the system (Figure 1). The final orientation of the frame into the current is also naturally facilitated by the tendency of the moored ship to head into the current. On touching the sea-bed, the weight hanging below the frame automatically releases the buoyant drift towards the free surface where it is recovered. The orientation of STRASS is later confirmed by a compass embedded in liquid gelatine that solidifies at water temperature. The system is recovered at the end of the sampling interval which in tidal environments should be preferably an integer number of tidal periods to determine the net transport rate. The recovery obviously requires fairweather conditions and care to maintain the frame horizontally to avoid loss of trapped sediment, unless the twelve traps can be closed at both ends by divers.

Immediately after recovery, the traps are removed from the racks and the trapped sediment is transferred to buckets. In the laboratory, the samples are sieved on a square mesh to remove the finest classes of sediment in agreement with the range of applicability of the traps. A mesh size of 100 μm is used when the current did not exceed 1.1 m/s, a mesh size of 125 μm is used for a maximum current speed of 1.4 m/s. During this operation, the samples are washed thoroughly to remove excess salt. They are oven-dried at 50 °C and weighed. Grain size analyses of sediments are carried out with a laser grain size analyzer, Malvern Instruments Ltd. The distribution of sediment transport rates as a function of grain size is then determined.

FIELD TEST

A field trial using STRASS was carried out April 25, 1997 in the tide-dominated waters of the eastern English Channel at latitude 50°26′.175*N* and longitude 1°28′.135*E* (Figure 3). Figure 4 is a picture of STRASS being lifted up from the deck of the Research Vessel 'Côtes de la Manche' prior to deployment. This work was undertaken within the research project on beach-nearshore sediment mobility at Merlimont Beach, northern France. The deployment site was situated 6.5 km seaward of the coast and 2.5 km landward of the Battur sand bank in 15 m water depth. An echo sounder survey showed the bottom in this area to be featureless and flat. The bed sediment had a 350 μm median grain diameter and was composed of 1% silt and very fine sand, 14.5% fine sand, 64% medium sand, 18% coarse sand and 2.5% very coarse sand (Figure 5). Bottom sediment surveys of the southern part of the eastern English Channel conducted by VASLET *et al.* (1978) and AUGRIS *et al.* (1987, 1995) confirm this local texture. At a larger scale, these investigations reveal fine sand blending with silts in the nearshore area, coarser sand in the vicinity of the deployment site and fine sand on Battur sand bank (Figure 3).

The tide in the observation area is predominantly semi-diurnal with a mean spring tide range of 7 m. For this experiment characterized by fairweather conditions, STRASS was deployed during a spring tidal cycle, *i.e.* a 12.40-hour period. When lowering STRASS to the sea-bed, the current direction was ebbing 220° clockwise from North, which finally yielded an orientation of the system as shown in Figure 3, with racks A–C approximately aligned north-west south-east, and racks B–D south-west north-east.

Concurrent with STRASS deployment, a heavily weighted frame with two Marsh-McBirney 3.8 cm-diameter electromagnetic flowmeters mounted 0.62 and 0.94 m above the sea-bed was installed 300 m to the north-east of STRASS location. The measured 540s-averaged currents were rotary with an anti-clockwise ellipse (Figure 6). The maximum flood current was heading north-north east, the maximum ebb current south-south west, with amplitudes 0.5 m/s at the topmost elevation (Figure 6b) and 0.4 m/s at the lowermost elevation (Figure 6a).

Table 1 gives the mass of dry sand particles larger than 100 μm collected in each trap. Figure 7 shows vertical distributions of transport rates in units of dry weight of transported sand per unit area per tidal cycle in various directions. The general trend is a decrease in transport rates in a given direction with increase in elevation from the sea-bed, except for traps C characterized by a higher rate at the upper level than at the intermediate level. It should be added that the vertical gradients in the transport rates are markedly steeper in traps B and D, than in traps A and C.

The distributions of suspended sand transport rates with particle size larger than 100 μm are shown in Figure 8. At the bottom level, the peak contribution to the transport rates in all directions corresponds to particles 200 μm in diameter. At the top level, the peak decreases to 160 μm. The distribution of transport rates for traps A and C are distinguished by a reversal of the vertical gradient between elevations 2 (z = 0.64 m) and 3 (z = 0.92 m). The inversion is valid for particles larger than 125 μm for traps C, and for particles smaller than 200 μm for traps A. The distributions of transport rates for traps B and D are characterized by a constant vertical gradient for all particle sizes.

Vector summation of the different directional transport rates yields the corresponding net transport rates. Table 2 gives the modulus and direction from clockwise relative to the north of the net total sand transport rate at each level. The modulus of the net transport rate is larger at the bottom level and seems statiscally constant at the upper two levels. The great disparity in terms of direction is surprising and seems difficult to explain.

Finally, the distributions of modulus and direction of the net sand transport rates as a function of particle size are presented in Figure 9. These results confirm the disparity observed in Table 2 for the total net transport rate. It is seen that the net transport rates of fine sand are predominantly cross-shore, onshore at the top and bottom levels, offshore at the intermediate level. At the lower level, the maximum net transport rate orientated to the west is associated with particles 250 to 400 μm in diameter which are the dominant grain size fractions of bottom sediments in the vicinity of the measurement point (Figure 4).

DISCUSSION

Magnitude of Sediment Transport Over One Tidal Period

The vertical structure of time-integrated suspended sediment transport rates measured during the first trial of

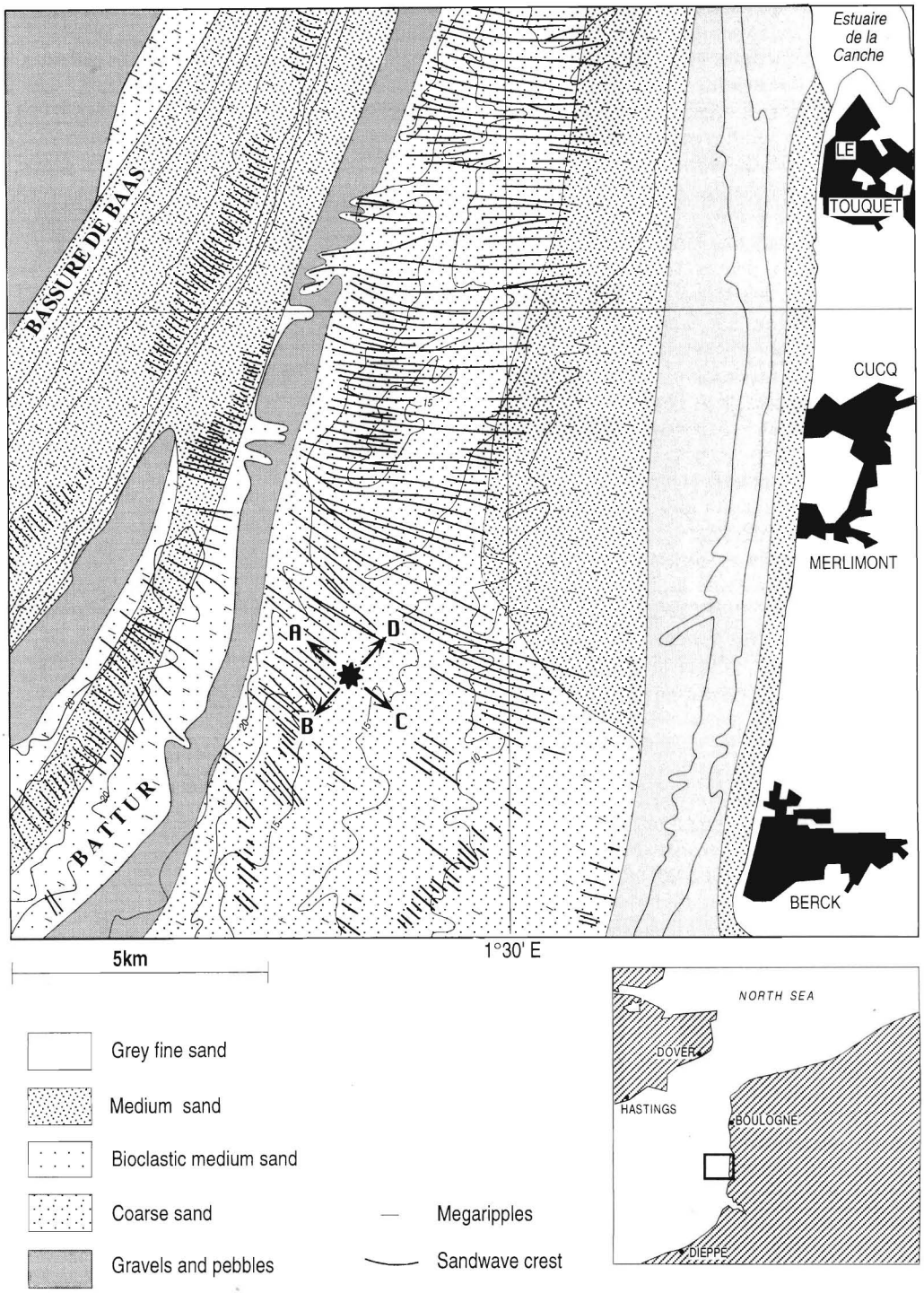

Figure 3. Site of STRASS measurement.

STRASS appears complicated in many ways. The first complication arises from the approximately equal mass of sediment captured in each rack of three traps (see Table 1), which is an intuitively surprising result. It is not evident in the first place to guess how much sediment should be collected in each trap when STRASS is immersed in a tidal current, because the angle that the instanteneous current makes with the four racks and the magnitude of the current are time-dependent functions.

A rough estimate of the theoretical amount of sediment

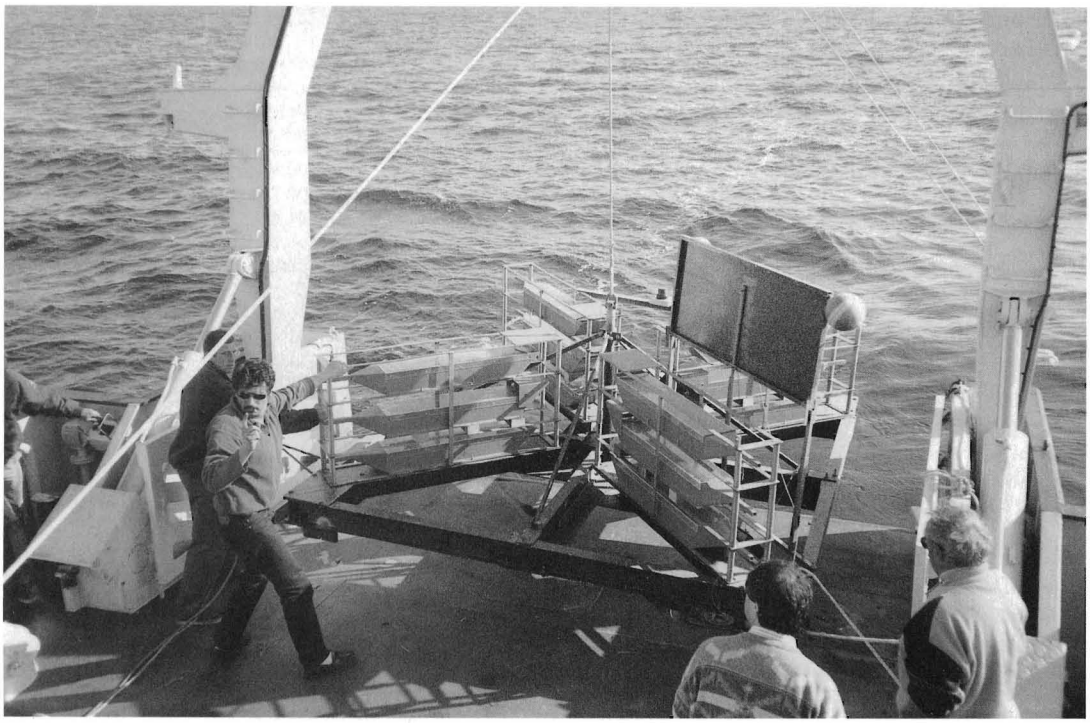

Figure 4. Picture of STRASS being lifted up from the deck of the Research Vessel 'Côtes de la Manche' prior to deployment.

that should be collected in each rack can be attempted. Figure 10 pictures the orientation of STRASS with respect to the tidal ellipse during the present deployment. The deployment did not occur when the flood or ebb current was fully established, which explains why racks B and D were not aligned with the major-axis of the current ellipse. Rack B was heading 220° from north, whereas the maximum ebbing current was heading 190° from north. The difference $\phi = 30°$ between the angles is of major importance to understand our measurements.

The total mass of sediment collected in any single trap over one tidal period T is given by

$$m = \int_0^T \left[\int_S C\mathbf{u} \cdot \mathbf{n} \, dS \right] dt \tag{1}$$

where C is the concentration of suspended sediment (kg/m^3), S the section of the intake nozzle and dS an infinitesimal portion of it, n the inward unit normal of the nozzle section, and u the ambient tidal current vector. We denote by (u, v)

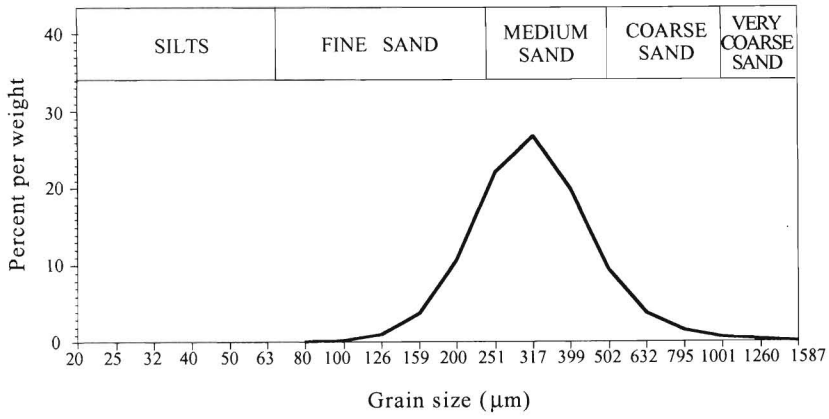

Figure 5. Grain-size frequency distribution of sea-bed sediments at the measurement site.

the horizontal velocity components along the minor and major axes of the current ellipse and by (u', v') the velocity components along racks A–C and B–D respectively (see Figure 10). The time evolution of (u, v) through a tidal cycle is approximately

$$u = U_0 \cos \omega t, \tag{2}$$

$$v = U_1 \sin \omega t, \tag{3}$$

with U_0 and U_1 the semi-minor and semi-major axes of the current ellipse, $\omega = 2\pi/T$, and with the time origin $t = 0$ corresponding to summit S of the current ellipse in Figure 10. The components (u', v') are deduced from (u, v) by a planar rotation of angle $-\phi$. Assuming an optimal angular trapping efficiency, it is clear that sediment convected by the tidal current will be collected in trap B when $v' > 0$, in trap D when $v' < 0$, in trap A when $u' > 0$, and in trap C when $u' < 0$. Considering for instance the total amount of sediment collected in trap B through one tidal cycle, Equation 1 together with condition $v' > 0$ gives

$$m_B = \int_{t_0}^{t_0 + (\pi/\omega)} \left[\int_S Cv' \, dS \right] dt, \tag{4}$$

where $\omega t_0 = -\arctan[(U_0/U_1)\tan \phi]$. In a very simplistic approach, with a suspended sediment concentration assumed spatially uniform and constant in time, the current ellipse symmetry implies that $m_B = m_D$ and $m_A = m_C$. Elementary algebra yields the final results,

$$m_B = m_D = \frac{2SC}{\omega}(U_0 \sin \phi \sin \theta_0 + U_1 \cos \phi \cos \theta_0), \tag{5}$$

$$m_A = m_C = \frac{2SC}{\omega}(U_0 \cos \phi \sin \theta_1 + U_1 \sin \phi \cos \theta_1), \tag{6}$$

in which angles θ_0 and θ_1 are given by

$$\theta_0 = \arctan\left(\frac{U_0}{U_1}\tan \phi\right) \tag{7}$$

$$\theta_1 = \arctan\left(\frac{U_0}{U_1}\frac{1}{\tan \phi}\right) \tag{8}$$

Considering Figure 6b of the present deployment, we had $U_0 = 0.1$ m/s, $U_1 = 0.5$ m/s, and $\phi = 30°$. This means that the masses of sediment collected in trap A3 (or C3) and in trap B3 (or D3) should have been in the ratio

$$\frac{m_B}{m_A} \simeq \frac{m_D}{m_C} \simeq 1.6 \tag{9}$$

The experimental ratio $m_B/m_A \simeq 1$ differs from (9) by 60%. On account of the over-simplifications of the theoretical analysis, the difference between measurements and predictions appears reasonable. It should be pointed out that with traps B and D exactly aligned with the major axis of the current ellipse, *i.e.* with $\phi = 0°$, the above ratio would become

$$\frac{m_B}{m_A} = \frac{U_1}{U_0} \simeq 5, \tag{10}$$

i.e. 3 times more than with the value for $\phi = 30°$.

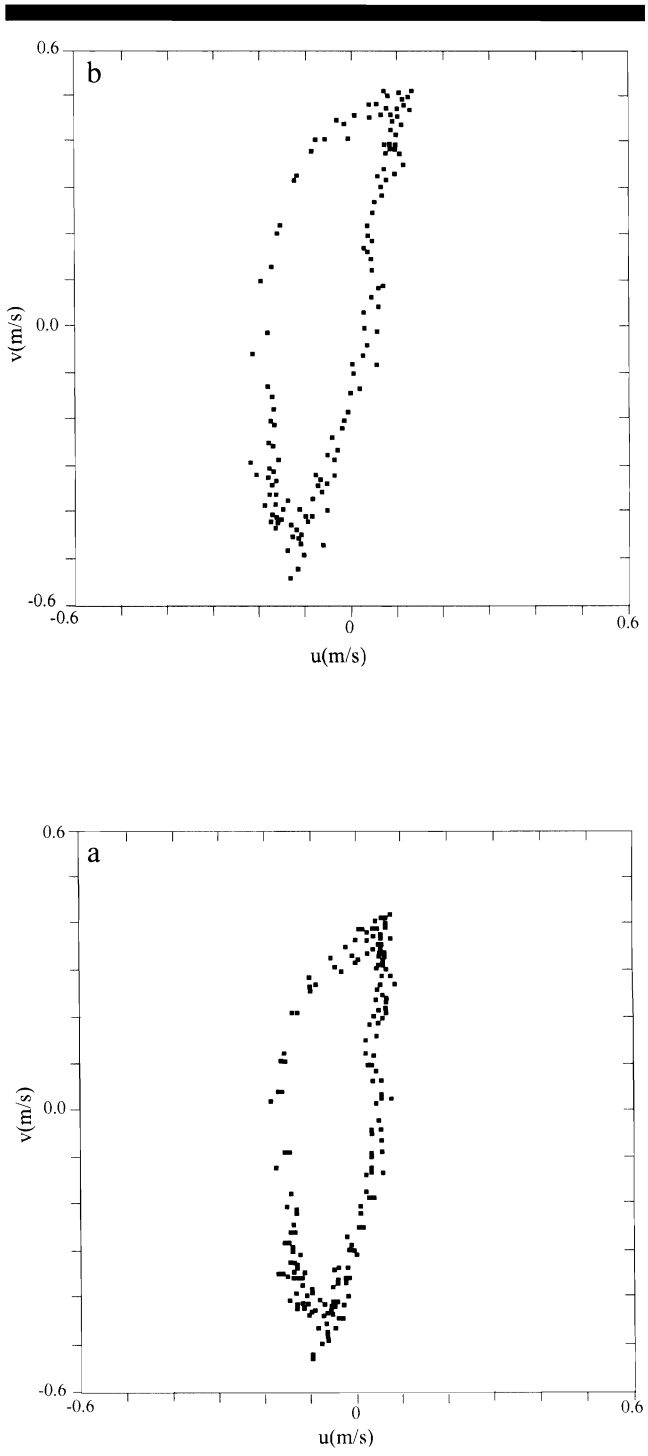

Figure 6. Tidal current ellipses from electromagnetic current meters at two elevations above the sea-bed during STRASS deployment. (a) z = 0.62 m; (b) z = 0.94 m.

Given the calm weather conditions of the present deployment, with little wave activity, we can see no other possible candidate than the tidal current for being responsible of sediment advection. We can speculate that the above 60% dis-

Table 1. *Masses of dry sand particles larger than 100 μm collected in the different traps. Figures 1, 2, 3 refer, respectively, to the lower, intermediate and upper levels.*

Trap Number	Mass of Trapped Sediment (g)
A1	77.90
A2	47.80
A3	46.15
B1	71.34
B2	52.82
B3	41.03
C1	83.10
C2	43.66
C3	50.80
D1	81.50
D2	55.22
D3	38.20

crepancy is the consequence of assuming in the analysis a spatially uniform and time-invariant concentration of suspended sediment C, the great complexity of the highly dynamic area characterized by non-equilibrium conditions making these assumptions questionable. In that respect, satellite observations have shown strong remote suspensions in the shallow fine sand areas to the west (Battur sand bank) and the east of STRASS (KERGOMARD *et al.*, 1993). This is likely to explain larger than expected amounts of trapped sediment in racks A and C. Another reason which could be put forward is the directional sensivity of the traps. When the instantaneous current makes a large angle with a trap axis (say $\geq$ 60°), a fraction of sediment could be lost because of high turbulence intensities in the entrance of the intake nozzle. Unfortunately, no laboratory tests have been performed for a trap unaligned with the current, which raises doubts as to whether the efficiency would indeed collapse at large incidence angles. We are not in a position to quantify this effect.

Net Sediment Transport Over One Tidal Cycle

The net sediment transport is a second order quantity, and consequently is subject to high statistical bias, especially in the present case with a deployment through one single tidal period. In spite of this uncertainty and of the complexity of the area, we can identify

(1) A net longshore transport of coarse bottom sediments located to the north and to the south of STRASS induced by the dominant ebb and flood flows;

(2) A net cross-shore transport of fine sand, probably resuspended to the south-west and the north-east of STRASS, and henceforth advected by low-magnitude rotating currents.

SUMMARY AND CONCLUSIONS

A multi-directional and multi-level trapping system for measuring the horizontal transport rates of suspended sand in the bottom boundary layer has been developed. The novel system is named STRASS (System for TRApping Suspended Sediment), and consists of four orthogonal series of three suspended sediment traps installed on a heavy lander frame. The system was designed to operate in multi-directional unsteady currents, such as tidal currents of the European Continental shelf. The use of STRASS in wave-dominated environments is not recommended.

STRASS has been tested during a spring tidal cycle in a coastal zone of the eastern English Channel characterized by strong heterogeneity in terms of bottom sediments, bathymetry and hydrodynamics. The experiment demonstrated that the system could be deployed and recovered securely, and that it was able to trap sediment in the field. It is difficult to draw clear-cut conclusions from this first deployment, yet significant transport of particles larger than 100 μm in diameter within one meter above the sea-bed was observed. A simple theoretical analysis has shown that the directional sensitivity of STRASS was highly dependent on the orientation of the racks with respect to the dominant tidal currents. The equal

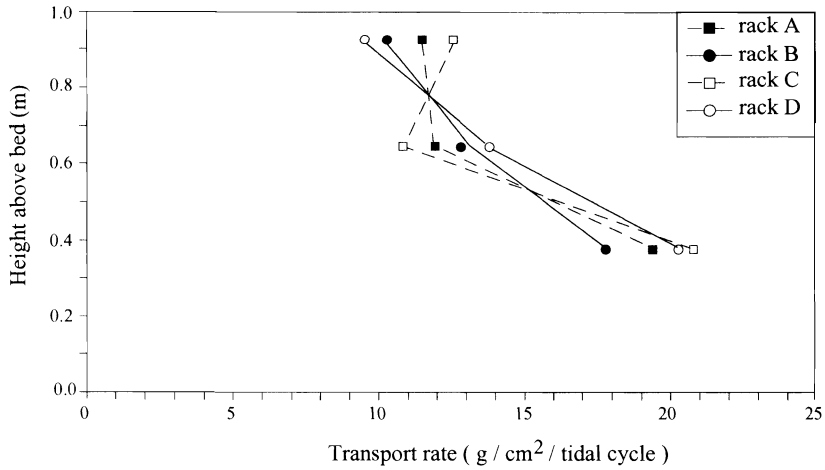

Figure 7. Vertical distributions of total suspended sand transport rates.

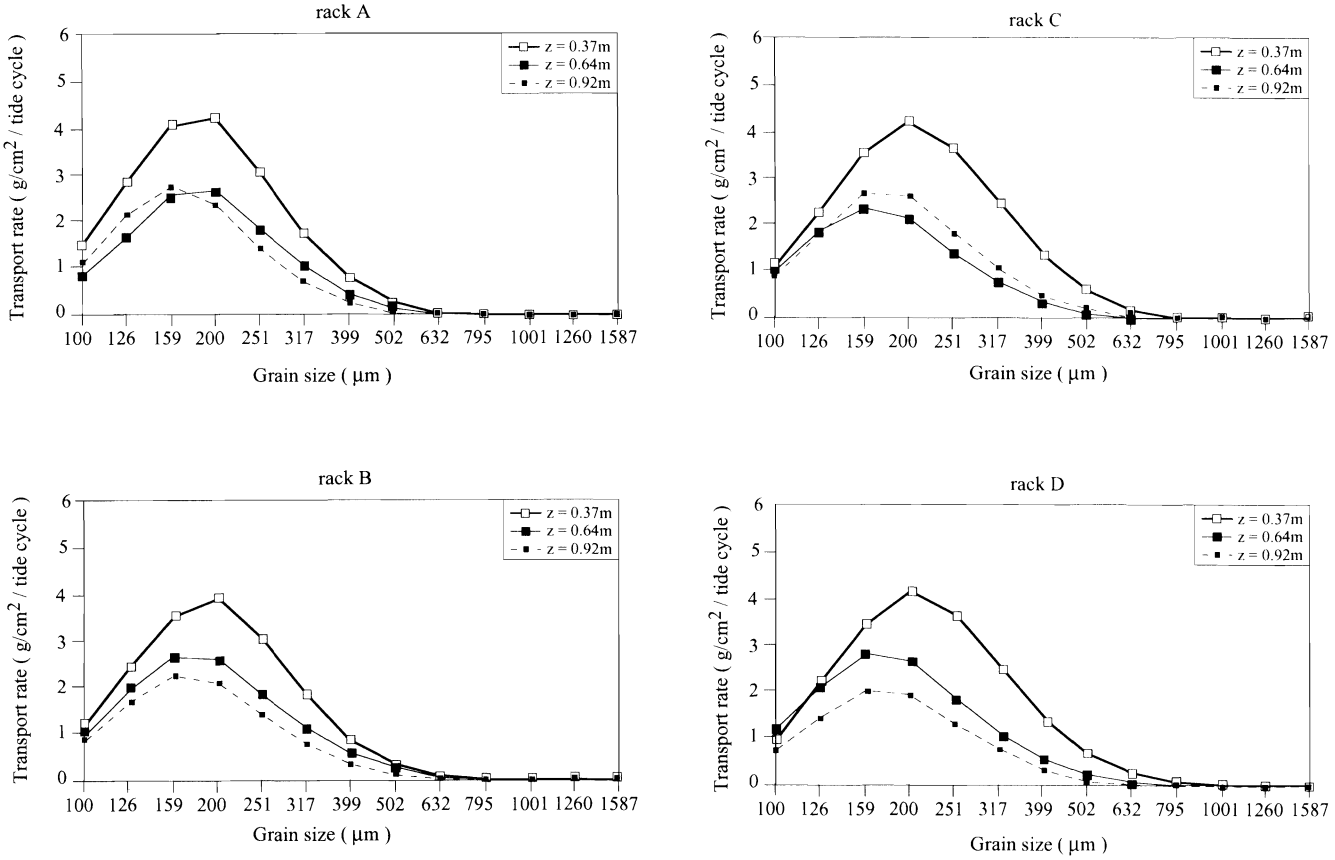

Figure 8. Distributions of suspended sand transport rates as against particle size in the different traps.

mass of sediment captured in the four orthogonal directions is not that far from what should be expected according to the simple theoretical approach. Concerning the net transport rates which are second order quantities, the present results could be interpreted as the consequence of the cross-shore heterogeneity of the application area in terms of hydrodynamics and sediment suspension.

After the first deployment, we acknowledge uncertainties remain about the efficiency of STRASS as a field instrument. These uncertainties lie essentially

(1) in the directional sensitivity of the traps

By this we mean: is the sediment trapping efficiency significantly altered at large incidence angles? This question remains unanswered for large incidence angles, yet less than 90°, since, due to their design, we are confident that the traps did not collect sediment coming from behind. To overcome this potential deficiency, we recommend that STRASS should be deployed at times of maximum flowing or ebbing current in tide-dominated environments, i.e. racks B and D exactly aligned with the major-axis of the current ellipse;

(2) in the experiment duration restricted to only one tidal cycle

Future field tests should be scheduled over several tidal cycles, especially at spells of spring or neap tides when the tidal range does not change too rapidly. This would reduce the statistical bias in the net transport rates;

(3) in the frame perturbation of the ambient flow

In that direction, we are quite confident that the individual traps have been designed correctly to minimize flow perturbations, the long intake nozzle playing here an important rôle. The perturbation of the lander frame seems to us a more significant point of worry, and it must be admitted that scour probably occurs around the structure during deployment. What can be said at this stage is that precautions have been taken to facilitate flow circulation within the frame. The square base is clear of the sea bed. In addition, racks A and C (or B and D) are not on the same line but shifted.

Finally, in view of the present results of STRASS and its

Table 2. *Modulus and direction clockwise relative to the north of the net total sand transport rates at the three levels.*

	Modulus (g/cm²/tidal cycle)	Direction (° clockwise/N)
Level 1	2.85	247
Level 2	1.20	160
Level 3	1.36	341

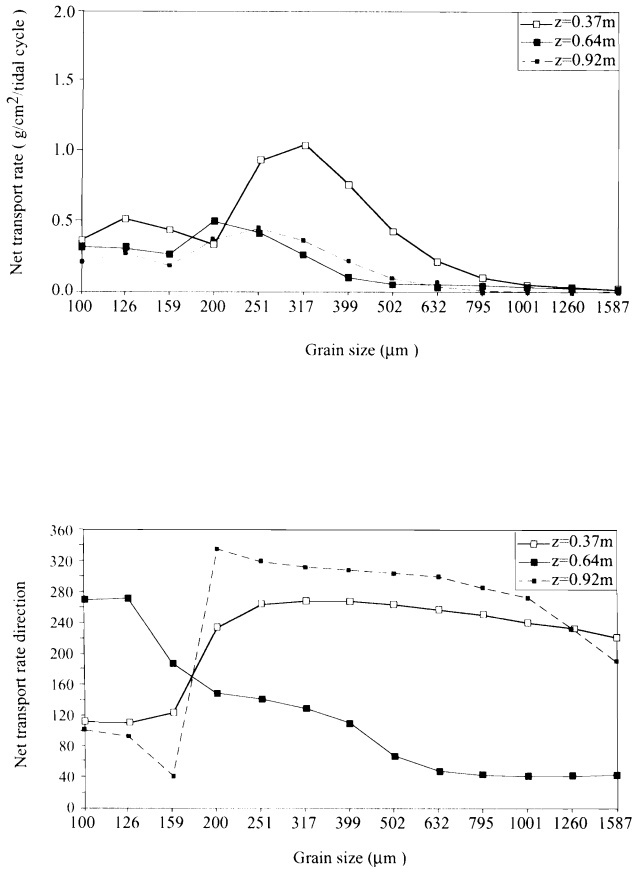

Figure 9. Modulus and direction relative to the north of the net sand transport rates against particle size at the three levels.

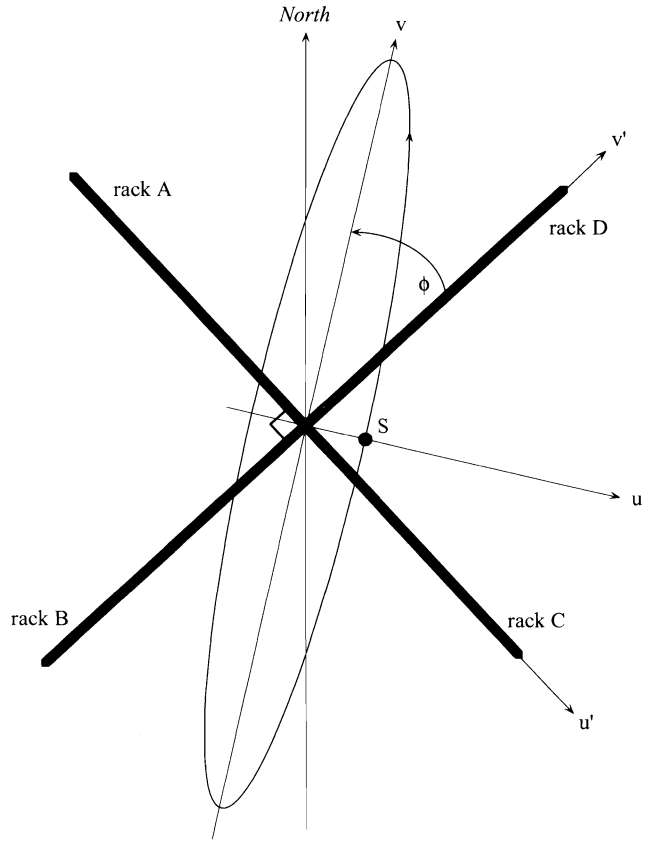

Figure 10. Schematic view of STRASS orientation with respect to the tidal current ellipse.

moderate cost of replication, this system offers an interesting solution for studying the spatial variability of suspended sediment transport rates in the coastal zone.

ACKNOWLEDGEMENTS

This work was carried out as part of the research programme 'DYnamique du Système COtier du Pas-de-Calais' (DYSCOP) supported by the Nord-Pas de Calais Regional Council, the European programme FEDER, the Centre National de la Recherche Scientifique (CNRS), and the French Ministry of Universities and Research (Grant DYSCOP-USTL999-2641-9385-907-9504-x). The authors wish to thank the Institut National des Sciences de l'Univers (INSU-CNRS) for supplying ship facilities (Research Vessel 'Côtes de la Manche'). Constructive help from the captain and the crew of the Research Vessel 'Côtes de la Manche' has been appreciated during deployment. Thanks are also due to A. Depuydt for his technical assistance to build STRASS, P. Recourt and D. Malengros for the laboratory analyses carried out on collected sediments, and M. Bocquet and J. Carpentier for the drawings and the picture of STRASS. The authors are indebted to Pr. Edward Anthony for useful discussions and suggestions which have contributed to improve the manuscript.

LITERATURE CITED

AUGRIS, C.; CLABAUT, P.; DEWEZ, S., and AUFFRET, J.-P., 1987. Surficial sediments map off Boulogne-sur-Mer (France). (1/43 600). Publication conjointe de l'IFREMER et de la Région Nord-Pas de Calais.

AUGRIS, C.; CLABAUT, P., and TESSIER, B., 1995. The coastal area of Nord-Pas de Calais (France) surficial geology map. (1/100 000). Publication conjointe de l'IFREMER, de la Région Nord-Pas de Calais et de l'Université des Sciences et Technologies de Lille.

ANTSYFEROV, S.M.; BASINSKI, T., and PYKHOV, N.V., 1983. Measurements of coastal suspended sediment concentrations. *Coastal Engineering,* 7, 145–166.

BASINSKI, T., 1989. *Field Studies on Sand Movement in the Coastal Zone.* Instytut Budownictwa Wodnego, Polska Akademia Nauk, Gdansk, Poland, 297p.

BASINSKI, T. and LEWANDOWKI, A., 1974. Field investigations of suspended sediment. *Proceedings of the 14th International Conference on Coastal Engineering,* Copenhagen, Denmark, 1096–1108.

BECCHI, I.; BILLI, P., and TACCONI, P., 1981. Analysis of a simple suspended load integrating sampler. *Proceedings of the Symposium on Erosion and Sediment Transport Measurement,* Florence, Italy, 115–122.

CHAPALAIN, G., 1998. A simple mono-directional trap for measuring horizontal transport rates of suspended sediment. *Journal of Marine Environmental Engineering,* 4, 245–276.

FUKUSHIMA, H. and MIZOGUCHI, Y., 1958. Field investigation of suspended littoral drift. *Proceedings of the 11th Japanese Conference on Coastal Engineering,* JSCE, 1, 131–134.

GRAF, W.H., 1984. *Hydraulics of Sediment Transport.* Water Resources Publications, Littleton, Colorado, U.S.A.

HAY, A.E. and SHENG, J., 1992. Vertical profiles of suspended sand concentration and size from multifrequency acoustic backscatter. *Journal of Geophysical Research,* 97, (C10), 15661–15667.

HOM-MA, M.; HORIKAWA, K., and SONU, C., 1960. A study of beach erosion at the sheltered beaches of Katasai and Kamakura. *Coastal Engineering in Japan,* 3, 101–122.

HORIKAWA, K. (Ed.), 1988. Nearshore dynamics and coastal processes. *Theory, measurement and predictive models.* Tokyo, Japan: University of Tokyo Press, 522p.

HUNTLEY, D.A., 1982. *In situ* sediment monitoring techniques. A survey of the state of the art in USA. Canadian Coastal Sediment Study, *Report C2S2-1,* Ottawa, Canada, 35p.

JAMES, C.P. and BRENNINKMEYER, B.M., 1971. Sediment entrainment within bores and backwash. *Geoscience and Man.* 18, 61–68.

KAJIMA, R., 1980. Field experiment of suspended load in the surf zone. *Report N° 11, TR-79-2,* Tokyo, Japan; National Environment Research Center, pp. 116–124.

KATTORI, S., 1982. Measurement of sediment transport by streamer sand trap. *Report N° 16, TR-81-2,* National Environment Research Center, Tokyo, Japan, 138–141.

KATTORI, S., 1983. Field experiment of sediment transport by streamer sand trap. *Report N° 17, TR-82-1,* Tokyo, Japan: National Environment Research Center, pp. 110–117.

KERGOMARD, C.; DE LUCA, D.; DILLIGEARD, E., and SANTER, R., 1993. *Télédétection et optique marine.* Rapport DYSCOP, 22p.

KRAUS, N.C., 1987. Application of portable traps for obtaining point measurements of sediment transport rates in the surf zone. *Journal of Coastal Research,* 3(2), 139–152.

MCCAVE, I.N., 1979. Suspended sediment. *In:* DYER, K.R. (Ed.), *Estuarine Hydrography and Sedimentation,* Cambridge, U.K., Cambridge University Press, ESBA, pp. 131–185.

NAGATA, Y., 1964. Deformation of temporal pattern of orbital wave velocity and sediment transport in shoaling water, in breaker zone and on foreshore. *Journal of the Oceanographic Society of Japan,* 20, N° 57070.

SATO, O., 1957. Field experiments of sediment transport at Tomakomai Industrial Harbor. Report of field experiment at Tomakomai Industrial Harbor N°8.

SCHOONEES, J.S., 1991. Field measurements of suspended sediment concentrations in the surf zone at Walker Bay. *In:* SOULSBY, R. and BETTESS, R. (Eds.), *Sand transport in rivers, estuaries and the sea, Euromech 262,* Balkema, Rotterdam, The Netherlands, 131–138.

VASLET, D.; LARSONNEUR, C., and AUFFRET, J.-P., 1978. *Carte des dépôts superficiels de la Manche,* (1/500 000). B.R.G.M. Editions, Orléans, France.

☐ RÉSUMÉ ☐

On décrit un nouveau système de piège à sédiments permettant la mesure du transport horizontal de sable en suspension dans la couche limite de fond induite par des courants multi-directionnels et instationnaires. Un premier déploiement dans l'environnement peu profond dominé par la marée de la Manche orientale durant un cycle de marée a démontré l'utilité de ce nouveau système. Les quantités de sédiment piégées dans les différentes directions sont comparées aux estimations d'une simple approche théorique. Nous discutons ensuite l'applicabilité du nouveau système. Les transports nets totaux et les transports nets en fonction de la taille du sédiment s'avèrent complexes. Ils se caractérisent par des contributions transversales, perpendiculaires au trait de côte, sans doute liées à l'hétérogénéité transversale de la zone d'application en termes d'hydrodynamique et de charge sédimentaire en suspension.

Bien qu'il soit encore sujet à des incertitudes quant à la sensibilité directionnelle des pièges qu'il accueille, et quant aux perturbations hydrodynamiques qu'il induit, le nouveau système semble un outil prometteur pour des études futures du transport de sédiment en zone côtière.